

Solution-Processed, Ultrathin Solar Cells from CdCl_3^- -Capped CdTe Nanocrystals: The Multiple Roles of CdCl_3^- Ligands

Hao Zhang,^{†,§} J. Matthew Kurley,^{†,§} Jake C. Russell,[†] Jaeyoung Jang,^{†,||} and Dmitri V. Talapin^{*,†,‡}

[†]Department of Chemistry and James Franck Institute, University of Chicago, Chicago, Illinois 60637, United States

[‡]Center for Nanoscale Materials, Argonne National Laboratory, Argonne, Illinois 60439, United States

S Supporting Information

ABSTRACT: Solution-processed CdTe solar cells using CdTe nanocrystal (NC) ink may offer an economically viable route for large-scale manufacturing. Here we design a new CdCl_3^- -capped CdTe NC ink by taking advantage of novel surface chemistry. In this ink, CdCl_3^- ligands act as surface ligands, sintering promoters, and dopants. Our solution chemistry allows obtaining very thin continuous layers of high-quality CdTe which is challenging for traditional vapor transport methods. Using benign solvents, in air, and without additional CdCl_2 treatment, we obtain a well-sintered CdTe absorber layer from the new ink and demonstrate thin-film solar cells with power conversion efficiency over 10%, a record efficiency for sub-400 nm thick CdTe absorber layer.

Over the past 40 years, efforts to improve photovoltaics have taken crystalline silicon nearly to its theoretical limit.¹ Second-generation solar cells using direct gap semiconductors, such as CdTe, have developed to the stage of rivaling silicon.² Solution processing offers an efficient and economically viable route to thin-film CdTe solar cells. In particular, sintered CdTe thin film deposited from soluble CdTe nanocrystals (NCs) or “NC ink” has been proven effective as the absorber layer for CdTe solar cells.³ Similar to the commercial CdTe photovoltaics made by vacuum-based techniques,⁴ CdCl_2 treatment is critical for ensuring high efficiencies in solution-processed CdTe solar cells. It promotes the sintering of CdTe NCs into large grains and concurrently improves the carrier transport by doping the interfaces.³ A new ink comprising both the active materials (CdTe NCs) and sintering promoters (e.g., CdCl_2) would be desirable for a facile solution-based fabrication of highly efficient CdTe solar cells.

Our design of the new ink containing sintering promoters was inspired by new developments in NC surface chemistry. During the past decade, the colloidal NC field has witnessed the rapid progress of new classes of inorganic surface ligands,⁵ including the nucleophilic chalcogenides,⁶ halides and pseudohalides,⁷ and more elaborate multidentate chalcogenidometallates,⁸ halometallates,^{7a,9} and (poly)oxometallates.¹⁰ These inorganic surface ligands have significantly enhanced electronic coupling by decreasing interparticle distance, enabling efficient solution-processed field-effect transistors (FET),¹¹ photodetectors,^{11a} and solar cells.¹² More interestingly, inorganic surface ligands can introduce new functionalities to NCs. For instance, we recently demonstrated several

compositionally matched molecular solders by controlling the surface chemistry of semiconductor NCs and microparticles.¹³ These solders situated at the surface of grains, facilitating sintering and carrier transport across grain boundaries.

In this work, we harness chlorocadmate (CdCl_3^-) ligand chemistry to design a new CdTe NC ink for solution-processed solar cells (Scheme S1). In this ink, CdCl_3^- ligands play a dual role: (i) to replace the organic ligands on CdTe NCs and afford a high solubility of NCs in a suitable solvent; and (ii) to promote CdTe grain growth. CdTe NCs in this new ink can efficiently sinter and grow into large grains. Moreover, chloride ions provide selective electronic doping of grain boundaries that helps to separate charge carriers in CdTe solar cells. The strategy of introducing new functionalities to NCs by the surface chemistry is anticipated to be generally employed to many other NC-based applications.

Preparing the new ink involved the exchange of insulating, long hydrocarbon ligands with CdCl_3^- (Scheme S1). Spherical CdTe NCs (Figure 1c) were synthesized using tetradecylphosphonic acid (TDPA) according to reported methods.¹⁴ For ligand exchange, we combined CdTe NCs dissolved in hexane with a solution of NH_4CdCl_3 in *N*-methylformamide (NMF). These two immiscible phases were stirred until CdTe NCs transferred to NMF and formed a stable colloid (Figure 1a). After purification (see Supporting Information (SI)), the ligand-exchanged CdTe NCs can redisperse in several solvents, including NMF, propylene carbonate, and pyridine. The deployment of NH_4CdCl_3 as surface ligands for colloidal NCs was first reported by Dirin et al.^{9a} NH_4CdCl_3 -capped NCs were colloidally stable as CdCl_3^- (and other anions generated by self-ionization) bound to the NC surface and provided electrostatic repulsion to overpower the interparticle van der Waals attractive force. The binding of negatively charged CdCl_3^- anions to NC surface was confirmed by the negative ζ -potential (−34 mV, Figure S1) of NH_4CdCl_3 -capped CdTe NCs in propylene carbonate. Transmission electron microscopy (TEM) images (Figure 1d) indicated that NCs retained their size and morphology. The integrity of CdTe NC cores after ligand exchange was also demonstrated by the optical absorption spectra. The absorption spectra (Figure 1e) of CdCl_3^- -capped CdTe NCs of various sizes resembled those of TDPA-capped ones. The ligand exchange procedure using NH_4CdCl_3 can be extended to CdTe NCs with other organic surfactants or morphologies (e.g., oleate-capped CdTe

Received: March 29, 2016

Published: June 7, 2016

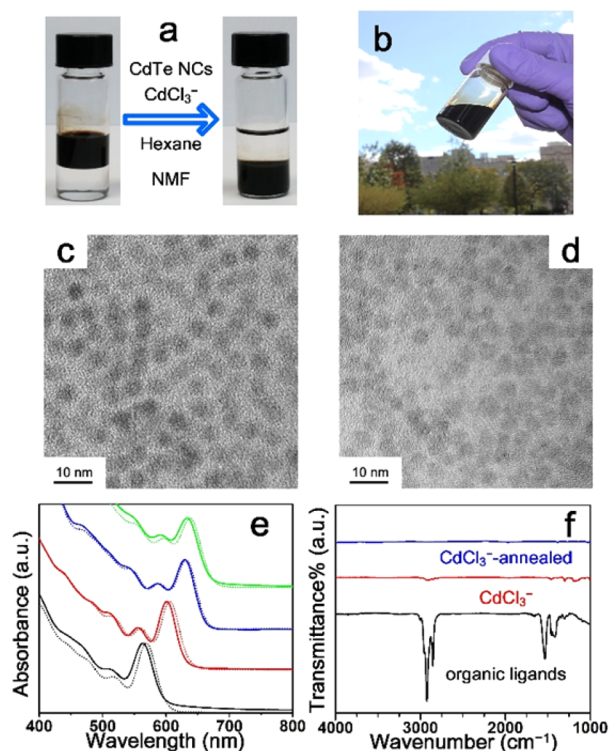


Figure 1. (a) A photograph showing the dark-colored CdTe NCs transferring from hexane to NMF in the presence of CdCl_3^- ligands. (b) A photograph of a concentrated CdCl_3^- -capped CdTe NC ink. (c,d) TEM images of CdTe NCs capped with tetradecylphosphonic acid and CdCl_3^- (NH_4CdCl_3) ligands, respectively. (e) UV-vis spectra of CdTe NCs with various sizes capped with tetradecylphosphonic acid (dotted lines) and CdCl_3^- ligands (solid lines). (f) FTIR spectra of CdTe NCs capped with native oleate ligands and CdCl_3^- through a large-scale ligand exchange.

tetrapods) and, more importantly, performed on a large scale. An ink containing several grams of CdCl_3^- -capped CdTe NCs can be made in a single batch (Figure 1b). The completeness of ligand exchange on such a large scale was monitored by Fourier transform infrared (FTIR) spectroscopy. The vibrational peaks observed in FTIR (Figure 1f) arising from native organic ligands (e.g., $2800\text{--}3000\text{ cm}^{-1}$ for C–H stretching mode, $1300\text{--}1500\text{ cm}^{-1}$ for C–H bending) were drastically suppressed in NCs with CdCl_3^- ligands. The weak IR features for CdCl_3^- -capped CdTe NCs could be assigned to solvent residue and counterions, as they disappeared after mild annealing ($200\text{ }^\circ\text{C}$ under vacuum). Besides NH_4CdCl_3 , CdCl_3^- moieties with other cations can also behave as ligands for CdTe NCs. For instance, reacting an equimolar mixture of CdCl_2 and pyridinium hydrochloride in NMF resulted in soluble species containing CdCl_3^- and $\text{C}_5\text{H}_5\text{NH}^+$. CdTe NCs capped with this compound (further referred to as pyrHCdCl_3) showed similar UV-vis absorption features to those capped with NH_4CdCl_3 (Figure S2). Moreover, pyrHCdCl_3 allowed a higher solubility (up to 150 mg/mL) of CdTe NCs in low boiling point solvents (pyridine, its mixture with alcohols, and nearly pure alcohols with several percent pyridine), which was crucial for the solution-based fabrication of high-quality CdTe thin films.

In this new ink, the surface-bound CdCl_3^- molecules play a vital role as the grain growth promoter of CdTe NCs. CdTe NCs before and after CdCl_3^- ligand exchange showed significantly different sintering behavior (Figures 2 and S3).

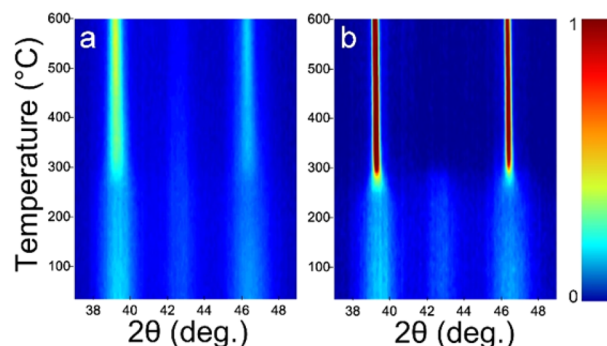


Figure 2. 2D intensity contour plots of in situ XRD patterns of CdTe NCs with (a) pyridine ligands and (b) pyrHCdCl_3 ligands as a function of temperature. Blue color indicates low XRD intensity, while red color corresponds to high intensity.

Broad peaks (centered at $\sim 39^\circ$, $\sim 42.5^\circ$, and 46.5°) with low intensities (as indicated by the blue color, Figures 2 and S3e) were observed in the case of as-synthesized CdTe NCs, corresponding to small CdTe grains (diameter about 5 nm). The native organic ligands inhibited the sintering of NCs, even at high temperatures, as indicated by the minor changes in intensities and widths of XRD peaks (Figure S3e). Exchanging native oleate ligands for pyridine did not result in a significant promotion of CdTe grain growth upon the heat treatment (Figure 2a). In contrast, the grain growth in CdCl_3^- -capped CdTe NCs was considerably enhanced, as evidenced by the high intensities (red color) and narrowing of the XRD peaks starting from $\sim 250\text{ }^\circ\text{C}$ (Figure 2b). Concomitantly, a characteristic peak for wurtzite phase ($\sim 42.5^\circ$) disappeared, indicating a complete transition to zinc-blende phase. As further evidence of grain growth, scanning electron microscopy (SEM) images of an annealed, single-layer CdTe film deposited from CdCl_3^- -capped CdTe NC ink revealed a uniform film of well-connected, sintered CdTe grains (Figure S3). Cross-sectional SEM (Figure 3a) of the complete CdTe device also showed a CdTe layer composed of sintered grains comparable in size to the thickness of the entire absorber film.

Prior to the design of CdCl_3^- -capped CdTe NC ink, we attempted to use CdTe NCs with several other inorganic surface ligands, including Cl^- , Te^{2-} , and CdTe_2^{2-} .^{6,7,13b} The simple halide, Cl^- , failed to afford highly concentrated, stable colloidal solution of CdTe NCs (solubility $<30\text{ mg/mL}$), which is a prerequisite for solution-processed solar cells. CdTe NCs capped with Te^{2-} and CdTe_2^{2-} sintered after annealing without CdCl_2 treatment, but had been too air sensitive. Besides, adding CdCl_2 to pyridine-exchanged CdTe NCs (or “additive approach”, see SI) was unable to remove the organic ligands and led to poor device performance (Figures S4 and S5 and related discussions). In comparison, the robust CdCl_3^- -capped CdTe NC ink in a mixture of pyridine and 1-propanol can be processed in air and produced high-quality CdTe layers using a layer-by-layer approach without additional CdCl_2 treatment. By using a device architecture outlined in Figure 3a and current/light soaking,^{3c} we achieved solar cells with $\sim 350\text{ nm}$ thick CdTe absorber showing PCE 10.3% with short-circuit current density (J_{SC}), open-circuit voltage (V_{OC}), and fill factor (FF) of $\sim 21\text{ mA/cm}^2$, $\sim 690\text{ mV}$, and $\sim 70\%$, respectively (Figure 3b and Table S1). The average values achieved were $\sim 9\%$, $\sim 20\text{ mA/cm}^2$, $\sim 670\text{ mV}$, and $\sim 68\%$ for PCE, J_{SC} , V_{OC} , and FF, respectively (Table S1). The photocurrent collected on each single CdTe solar cell device (area: 8 mm^2) was generated by

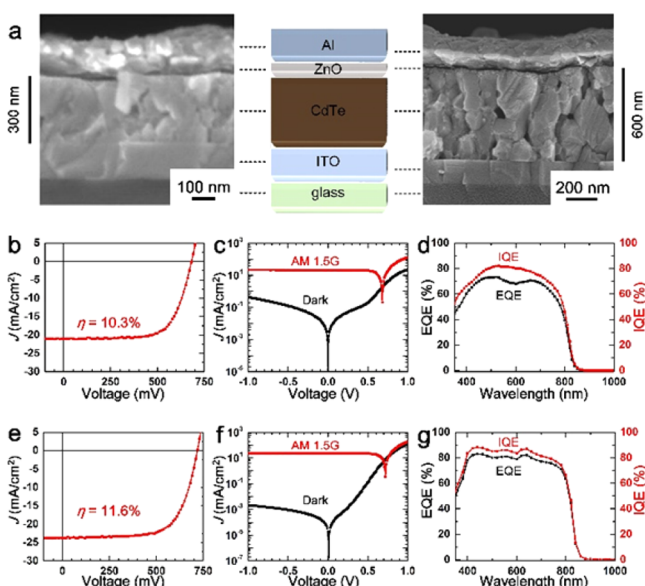


Figure 3. (a) Schematic and cross-sectional SEM image of complete CdTe solar cell devices made from CdCl₃⁻-capped CdTe NC ink with (left) ~350 and (right) 600 nm-thick CdTe layers. (b–g) Device characteristics for CdTe solar cells with (b–d) ~350 and (e–g) 600 nm-thick CdTe active layers, respectively. (b,e) Current density–voltage (*J*–*V*) curve under AM 1.5G illumination. (c,f) Light and dark *J*–*V* curves and (d,g) EQE and IQE spectra for the solar cells shown as black and red curves, respectively.

an incident light exposed to an area of 6 mm² using an aperture mask. The external quantum efficiency (EQE) spectrum (Figure 3d) matched well with the measured *J*_{SC}. Internal quantum efficiency (IQE) (Figure 3d) was about 10% higher compared to EQE values, consistent with an estimate for light reflection at the air/glass interface. These reasonably high PCE values compared favorably with devices with very thin CdTe layers. Traditional CdTe solar cells use several micron-thick CdTe layers, which poses obvious concerns given Te scarcity and Cd toxicity issues. Solution deposition can be easily scaled to different film thickness as shown in Figure 3a by simply adjusting the concentration of NC ink and the number of deposited layers. For example, the solar cells with ~600 nm thick CdTe layer showed PCE 11.6% due to improvements in both *J*_{SC} (23.7 mA/cm²) and *V*_{OC} (718 mV) with FF 68% (Figure 3e–g and Table S1). Extensive studies of sputtered ultrathin CdTe solar cells demonstrated optimized 11% PCE for 0.5 μm CdTe layer and 8% record efficiency for devices with 0.25 μm CdTe due to shunting and incomplete light absorption.¹⁵ Switching from gas phase to solution deposition clearly helps to improve the uniformity of ultrathin CdTe layers (Figure 3a) resulting in 10% PCE for devices with sub-400 nm absorber. We anticipate the room for further improvements through the optimization of device stack and deposition conditions, e.g., by annealing the CdTe layers not in air but under controlled atmosphere.

In a series of control experiments, we compared performance of CdTe solar cells made of CdTe NCs capped with the pyrHCdCl₃ surface ligands and of the same batch of NCs but capped with pyridine. In the latter case, each spin-coated NC layer was soaked in a saturated solution of CdCl₂ in methanol at 60 °C before annealing at 350 °C.^{3b,c} We noted that at comparable thickness of CdTe absorber layers, the solar cells made with pyrHCdCl₃ surface ligands showed comparable or

higher PCE values primarily originated from a significant increase in *V*_{OC} (Table S1). This difference in *V*_{OC} can be ascribed to a better passivation of grain boundaries and reduced Shockley–Read–Hall recombination velocity in the CdTe layer.^{3c}

The ability to integrate the grain growth promoter in form of the surface ligands for CdTe NCs made our new ink compatible with high-throughput deposition methods, such as spray coating or doctor blading. In preliminary tests for spray-coated solar cells, we achieved PCE (8–9%, Table S1) comparable to spin-coated devices, using CdCl₃⁻-capped CdTe NC ink in methanol with a small amount of pyridine. This suggested the possibility of high-throughput, roll-to-roll large area deposition of CdTe layers by using the new ink on various substrates.

Inspired by the successful design of CdCl₃⁻-capped CdTe NC ink, we envisage a wide variety of potential applications of hallometallate-capped II–VI NCs and their alloys. As a preliminary step, we utilized CdCl₃⁻-capped CdSe NCs to fabricate FET devices. Similar to the case of CdTe, CdSe NCs can disperse in NMF with NH₄CdCl₃ ligands without notable changes in the crystal size (Figure S7). CdCl₃⁻ ligands promoted the grain growth of NCs with respect to other ligands, such as I⁻. The sintered CdSe nanograins (~20 nm) showed decent electron mobility up to ~30 cm²/(V s), depending on the annealing temperature, estimated from the FET transfer characteristics (Figure S8). More interestingly, the air-stable CdCl₃⁻ ligands allowed the ligand exchange process and FET channel fabrication, for the first time, to be performed in air, resulting in CdSe FETs with preliminary mobilities of ~2–3 cm²/V·s.

In conclusion, we have designed an ink of CdCl₃⁻-capped CdTe NCs, which combines the photovoltaic active materials and the sintering promoters in a single solution. The dual role of CdCl₃⁻ ligands allows a facile device fabrication with no need for CdCl₂ treatment. Solar cells made from this new ink show high PCE over 10%. Furthermore, we envisage the chemical design of NC-based materials through inorganic ligand chemistry can be generally applied to a broad scope of materials and fields. Materials of interest include Hg_{1-x}Cd_xTe (MCT), Cd_{1-x}Zn_xTe (CZT), and other II–VI alloys. MCT alloys are the prevalent materials for infrared photodetectors, while CZT alloys are commonly used in high-energy photon detection, especially X- and γ-rays. The additional functionalities brought by surface ligands would contribute to better performance and improved manufacturing for NC-based devices in a wide variety of fields.

■ ASSOCIATED CONTENT

📄 Supporting Information

The Supporting Information is available free of charge on the ACS Publications website at DOI: 10.1021/jacs.6b03240.

Additional experimental details, figures, and tables as described in the text (PDF)

■ AUTHOR INFORMATION

Corresponding Author

*dvtalapin@uchicago.edu

Present Address

^{||}Department of Energy Engineering, Hanyang University, Seoul 133–791, Republic of Korea.

Author Contributions

[§]These authors contributed equally.

Notes

The authors declare no competing financial interest.

ACKNOWLEDGMENTS

We thank Gregory Pach and Bobby To at National Renewable Energy Laboratory and Qiti Guo at Materials Research Science and Engineering Center at University of Chicago for the help with cross-sectional SEM images. This work was supported by the Department of Defense Office of Naval Research under grant no. N00014-13-1-0490, Air Force Office of Scientific Research under grant no. FA9550-14-1-0367, Department of Energy SunShot program under award no. DE-EE0005312, and by II–VI Foundation. The work used facilities supported by the NSF MRSEC Program under award no. DMR-14-20703.

REFERENCES

- (1) Green, M. A. *Semicond. Sci. Technol.* **1993**, *8*, 1.
- (2) (a) Romeo, A.; Terheggen, M.; Abou-Ras, D.; Bätzner, D. L.; Haug, F.-J.; Kälin, M.; Rudmann, D.; Tiwari, A. N. *Prog. Photovoltaics* **2004**, *12*, 93. (b) (a) Gur, I.; Fromer, N. A.; Geier, M. L.; Alivisatos, A. P. *Science* **2005**, *310*, 462. (b) Jasieniak, J.; MacDonald, B. I.; Watkins, S. E.; Mulvaney, P. *Nano Lett.* **2011**, *11*, 2856. (c) Panthani, M. G.; Kurley, J. M.; Crisp, R. W.; Dietz, T. C.; Ezzayat, T.; Luther, J. M.; Talapin, D. V. *Nano Lett.* **2014**, *14*, 670. (d) Crisp, R. W.; Panthani, M. G.; Rance, W. L.; Duenow, J. N.; Parilla, P. A.; Callahan, R.; Dabney, M. S.; Berry, J. J.; Talapin, D. V.; Luther, J. M. *ACS Nano* **2014**, *8*, 9063. (e) Townsend, T. K.; Heuer, W. B.; Foos, E. E.; Kowalski, E.; Yoon, W.; Tischler, J. J. *Mater. Chem. A* **2015**, *3*, 13057.
- (4) Major, J. D.; Treharne, R. E.; Phillips, L. J.; Durose, K. *Nature* **2014**, *511*, 334.
- (5) Boles, M. A.; Ling, D.; Hyeon, T.; Talapin, D. V. *Nat. Mater.* **2016**, *15*, 141.
- (6) Nag, A.; Kovalenko, M. V.; Lee, J.-S.; Liu, W.; Spokoyny, B.; Talapin, D. V. *J. Am. Chem. Soc.* **2011**, *133*, 10612.
- (7) (a) Zhang, H.; Jang, J.; Liu, W.; Talapin, D. V. *ACS Nano* **2014**, *8*, 7359. (b) Norman, Z. M.; Anderson, N. C.; Owen, J. S. *ACS Nano* **2014**, *8*, 7513. (c) Ning, Z.; Dong, H.; Zhang, Q.; Voznyy, O.; Sargent, E. H. *ACS Nano* **2014**, *8*, 10321. (d) Fafarman, A. T.; Koh, W.-K.; Diroll, B. T.; Kim, D. K.; Ko, D.-K.; Oh, S. J.; Ye, X.; Doan-Nguyen, V.; Crump, M. R.; Reifsnnyder, D. C.; Murray, C. B.; Kagan, C. R. *J. Am. Chem. Soc.* **2011**, *133*, 15753.
- (8) (a) Kovalenko, M. V.; Scheele, M.; Talapin, D. V. *Science* **2009**, *324*, 1417. (b) Kovalenko, M. V.; Bodnarchuk, M. I.; Zaumseil, J.; Lee, J.-S.; Talapin, D. V. *J. Am. Chem. Soc.* **2010**, *132*, 10085.
- (9) (a) Dirin, D. N.; Dreyfuss, S.; Bodnarchuk, M. I.; Nedelcu, G.; Papagiorgis, P.; Itskos, G.; Kovalenko, M. V. *J. Am. Chem. Soc.* **2014**, *136*, 6550. (b) Ning, Z.; Gong, X.; Comin, R.; Walters, G.; Fan, F.; Voznyy, O.; Yassitepe, E.; Buin, A.; Hoogland, S.; Sargent, E. H. *Nature* **2015**, *523*, 324.
- (10) (a) Llordes, A.; Garcia, G.; Gazquez, J.; Milliron, D. J. *Nature* **2013**, *500*, 323. (b) Huang, J.; Liu, W.; Dolzhenkov, D. S.; Protesescu, L.; Kovalenko, M. V.; Koo, B.; Chattopadhyay, S.; Shevchenko, E. V.; Talapin, D. V. *ACS Nano* **2014**, *8*, 9388.
- (11) (a) Lee, J.-S.; Kovalenko, M. V.; Huang, J.; Chung, D. S.; Talapin, D. V. *Nat. Nanotechnol.* **2011**, *6*, 348. (b) Choi, J.-H.; Fafarman, A. T.; Oh, S. J.; Ko, D.-K.; Kim, D. K.; Diroll, B. T.; Muramoto, S.; Gillen, J. G.; Murray, C. B.; Kagan, C. R. *Nano Lett.* **2012**, *12*, 2631. (c) Kim, D. K.; Lai, Y.; Diroll, B. T.; Murray, C. B.; Kagan, C. R. *Nat. Commun.* **2012**, *3*, 1216.
- (12) Ning, Z.; Voznyy, O.; Pan, J.; Hoogland, S.; Adinolfi, V.; Xu, J.; Li, M.; Kirmani, A. R.; Sun, J.-P.; Minor, J.; Kemp, K. W.; Dong, H.; Rollny, L.; Labelle, A.; Carey, G.; Sutherland, B.; Hill, I.; Amassian, A.; Liu, H.; Tang, J.; Bakr, O. M.; Sargent, E. H. *Nat. Mater.* **2014**, *13*, 822.
- (13) (a) Son, J. S.; Zhang, H.; Jang, J.; Poudel, B.; Waring, A.; Nally, L.; Talapin, D. V. *Angew. Chem., Int. Ed.* **2014**, *53*, 7466. (b) Dolzhenkov, D. S.; Zhang, H.; Jang, J.; Son, J. S.; Panthani, M. G.; Chattopadhyay, S.; Shibata, T.; Talapin, D. V. *Science* **2015**, *347*, 425. (c) Jang, J.; Dolzhenkov, D. S.; Liu, W.; Nam, S.; Shim, M.; Talapin, D. V. *Nano Lett.* **2015**, *15*, 6309.
- (14) Yu, W. W.; Qu, L.; Guo, W.; Peng, X. *Chem. Mater.* **2003**, *15*, 2854.
- (15) Paudel, N. R.; Wieland, K. A.; Compaan, A. D. *Sol. Energy Mater. Sol. Cells* **2012**, *105*, 109.